

Original Article

# Integrating ANFIS for Improved MPPT in A 24V PEMFC System with Switched Inductor Boost Converter

E. Kalaiyaran<sup>1</sup>, S. Singaravelu<sup>2</sup>

<sup>1,2</sup>Department of Electrical Engineering, Annamalai University, Tamilnadu, India.

<sup>1</sup>Corresponding Author : [kalaiyaran.a.m@gmail.com](mailto:kalaiyaran.a.m@gmail.com)

Received: 12 March 2024

Revised: 13 April 2024

Accepted: 10 May 2024

Published: 29 May 2024

**Abstract** - This study presents a comprehensive analysis of a 1.26 kW, 24V Proton Exchange Membrane Fuel Cell (PEMFC) system integrated with an Adaptive Neuro-Fuzzy Inference System (ANFIS) based Maximum Power Point Tracking (MPPT) control and a switched inductor DC-to-DC boost converter. The converter is designed to achieve an output voltage of 220V. The primary objectives of this research are to model the PEMFC system, design the switched inductor DC-to-DC boost converter and develop an ANFIS model for MPPT control. Simulations are conducted to observe the fuel cell voltage and current under varying air and water pressure conditions and the dynamics in the fuel cell parameters are analyzed. Additionally, the study investigates the impact of temperature variations on the fuel cell's performance. The converter output voltage and power are observed under Standard Test Conditions (STC) to evaluate the overall system efficiency. A key focus of the research is the comparison between the ANFIS-based MPPT control and Artificial Neural Network (ANN) based MPPT control for the Switched Inductor DC-to-DC Boost Converter (SIDC) output. The comparative analysis considers variations in air and water pressure as well as temperature changes. The results reveal insights into the dynamic behavior of the PEMFC system under different operating conditions. Furthermore, the comparative study between ANFIS and ANN highlights the efficacy of ANFIS in optimizing the converter output. The proposed model and control strategies contribute to the advancement of PEMFC technology, which offers a valuable foundation for the design and optimization of fuel cell systems in various environmental conditions. This research aligns with the growing interest in renewable energy sources and underscores the importance of advanced control strategies for enhancing the performance of fuel cell systems.

**Keywords** - PEMFC, ANFIS, MPPT, Temperature, Smart control.

## 1. Introduction

Scientists around the world are paying much attention to a special way of using electricity and carbon dioxide to make useful fuels. This method can help us deal with the global energy problem. The main idea is to create a kind of cycle where we can store chemical fuels like hydrogen and then turn them back into electricity when needed. This is done through a process called electrochemical reactions in devices called fuel cells [1].

The big challenge is to make this process work well and be environmentally friendly. Researchers are focusing on developing better materials, like special membranes and tiny particles called nanomaterials, which can make the conversion of fuels to electricity more efficient. They are also trying to reduce the use of expensive materials (platinum), which is currently used in a part of the fuel cell called the cathode [2]. By improving these technologies, scientists hope to create fuel cells that work at lower temperatures and are more efficient [3]. This could lead to cleaner and more sustainable energy solutions, helping us move towards a

future where we can produce and use energy in a way that is better for the environment.

PEMFC find applications in two main areas, namely transportation and portable power generation. These areas pose unique challenges in fuel cell design due to limitations in space, weight constraints and the need for rapid and dynamic power delivery. PEM fuel cells play a crucial role in electric passenger cars, utility vehicles and buses, which provide power in the range of 20 to 250 kW. The advantage lies in zero emissions, high energy conversion efficiency and a compact design suitable for automotive use [4].

Major automotive companies are actively working on advancing PEM fuel cell technology to address key commercialization challenges such as cost, durability and cold-start capability [5]. PEM fuel cells are employed to provide power for small portable electronics by offering a reliable and efficient energy source for devices like smartphones, laptops and other gadgets. PEM fuel cells are instrumental in addressing the energy needs of transportation



by offering clean and efficient power solutions for various vehicles. In the next 5-10 years, there is an expectation that Perfluoro Sulfonic Acid (PFSA)-based polymers, which are characterized by enhanced durability, will dominate the Proton Exchange Membrane (PEM) market. However, issues such as corrosion resistance, fabrication cost and interfacial contact resistance were the challenges that persist in Bipolar Plate (BP) design. Despite these challenges, the integrated BP-MEA (Membrane Electrode Assembly) design is anticipated to pave a promising path toward achieving ultrahigh power density in PEMFCs [7].

In the renewable energy landscape, PEMFCs play a pivotal role with significant importance. Their role extends beyond conventional energy sources, and their significance is underscored by their contributions to clean energy generation and adherence to environmental and sustainability considerations. PEMFCs play a pivotal role in clean energy generation, which benefits from nanotechnology to improve efficiency and sustainability.

Nanomaterials, like platinum nanoparticles, can enhance catalytic reactions by optimizing energy conversion. Nanostructured membranes and Gas Diffusion Layers (GDLs) improve durability and mass transport efficiency, which extends the lifespan of PEMFCs. Incorporating nanocomposite materials in electrolyte membranes ensures better water retention and ion conductivity. Nanostructured BP addresses corrosion challenges through innovative coatings and interfaces. Environmental benefits extend to reduced resource consumption and improved system efficiency through controlled nanoscale fabrication [8].

PEMFCs are highly sensitive to operating conditions, including temperature, pressure and humidity fluctuations. Changes in temperature impact reaction kinetics and material properties, while pressure variations affect mass transport and reactant distribution. Fuel composition alterations, particularly in hydrogen purity, may lead to catalyst degradation. Load fluctuations and transient operating states may create additional challenges [9]. Effective management of these diverse conditions is crucial for optimizing PEMFC performance to ensure durability and maintain stable power output.

MPPT holds paramount significance in enhancing the efficiency of energy extraction from renewable sources, particularly in systems like Proton Exchange Membrane Fuel Cells (PEMFCs). MPPT algorithms enable the continuous adjustment of operating points to capture the maximum available power from the fuel cell by optimizing the conversion process [10]. This adaptive control mechanism ensures that the system operates at the most favourable voltage and current levels by mitigating power losses and maximizing energy yield. The impacts of effective MPPT extend to the overall system efficiency, which contributes to

elevated power generation and improved response to varying environmental conditions. The Authors [11] discuss a comprehensive review of MPPT techniques for extracting maximum power from PEMFCs, which highlights significant parameters for performance evaluation. This thorough review enables researchers to compare and choose suitable MPPT techniques for specific PEMFC applications.

Converters play a crucial role in power electronics by enabling the efficient manipulation and control of electrical energy. Among these, dc-dc boost converters hold significance in voltage regulation and energy conversion processes. In the context of PEMFC stacks, the application of dc-dc boost converters is pivotal for ensuring optimal performance and energy conversion efficiency [12]. In fuel cell applications like automotive propulsion or stationary power generation, it is essential to employ DC-DC boost converters to elevate the voltage output and meet diverse operational requirements where fuel cells inherently produce a relatively low voltage.

The DC-DC boost converters, which are integrated into the fuel cell stack system, play a critical role in elevating the voltage level to meet the demands of downstream components. This is particularly crucial in electric vehicles or grid-connected systems where a stable and elevated voltage is necessary for continuous operation. The Authors [12] highlight the critical role of power converters in enhancing the overall performance and adaptability of fuel cell-based systems. The authors [12] also declare the importance of selecting the right power converter architecture and technology, which is underscored to emphasize the potential for efficiency, compactness and modularity in the output power interface by ensuring thermal compatibility with different integration methods into global fuel cell-based power sources.

The Authors [13] highlight the ongoing challenges in commercializing PEMFCs despite their high energy density and significant research and development interest. Classical Proportional Integral and Derivative (PID) controllers are commonly employed for feedback voltage control and feed-forward current control by adjusting hydrogen and airflow rates. Self-tuning adaptive PID controllers and sliding mode controllers were highlighted for their ability to adapt to changing dynamics and faster response. The use of Model Predictive Control (MPC) in a PEMFC model for predicting system behavior and updating controller action is also discussed. Notably, the Authors [13] emphasize the recent integration of artificial intelligence techniques, including Neural Network Control (NNC), Fuzzy Logic Control (FLC) and FLC-PID control in PEMFC system control.

Adaptive Neuro-Fuzzy Inference System (ANFIS) and Artificial Neural Network (ANN) are two powerful computational models that blend the strengths of fuzzy logic

and neural networks to address complex problems in diverse fields. The Authors [14] demonstrate the successful application of ANN and ANFIS as MPPT controllers to enhance the performance of a standalone photovoltaic system. The successful application of ANN and ANFIS as MPPT controllers in enhancing the performance of a standalone photovoltaic system prompts the consideration of applying similar control strategies to PEMFCs. The adaptability and robust performance of these controllers in the photovoltaic context suggested that they could be valuable tools in optimizing PEMFC control systems.

This study identifies limitations in existing control and converter technologies employed in PEMFC systems. These limitations could pertain to the efficiency of control strategies, adaptability to varying operating conditions and the overall effectiveness of converter technologies. Investigating these limitations is crucial for developing advanced control systems and converters that can address the specific needs and challenges of PEMFC technology. It is important to develop and implement control strategies to increase PEMFC system stability and maximize energy conversion.

This research objective is to establish comprehensive approaches to optimize the overall performance of PEMFC systems. Integration of advanced control and converter technologies will create a more robust and adaptive PEMFC system. By addressing these research objectives, the study aims to bridge the identified research gap, which contributes to the advancement of PEMFC technology and overcoming current challenges in control and converter technologies.

The workflow with the PEMFC System Configuration with a detailed description and an overview of the switched inductor DC-to-DC boost converter. The objective of this work is to model the PEMFC system, design the switched inductor DC-to-DC boost converter and develop an ANFIS model for improved MPPT control. In the Simulation Setup phase, MATLAB/Simulink is utilized to establish parameters and conditions for simulations, which provides a versatile platform for modeling and evaluating the dynamic behavior of the 1.26 kW, 24V PEMFC system and the switched inductor DC-to-DC boost converter.

The subsequent Dynamic Analysis stage involves observing fuel cell voltage and current under varying air and water pressure, as well as assessing the impact of temperature variations on fuel cell performance. Converter Output Analysis at STC is conducted to examine the converter's output voltage and power. Finally, a comparative analysis is carried out by comparing ANFIS-based MPPT with ANN based MPPT for analyzing variations in air and water pressure along with temperature effects. The workflow concludes with the results and insights section, summarizing key findings and drawing conclusions from the conducted analyses.

## 2. System Configurations

### 2.1. Design and Simulation of 1.26 kW, 24V PEMFC Stack

The operational temperature significantly impacts the performance of a fuel cell with a deviation affecting both efficiency and power generation. Excessive heat can lead to decreased efficiency and power output while operating at higher temperatures can enhance the utilization of residual heat. Optimal temperature management is crucial to operate fuel cells most effectively within a specific temperature range.

Achieving and maintaining this ideal temperature is supreme for ensuring the fuel cell's reliability and optimal performance. In the search for sustainable and efficient energy solutions, PEMFCs have emerged as a cutting-edge technology by utilizing the chemical energy of hydrogen to generate electricity with remarkable efficiency and minimal environmental impact.

Substantial research efforts have been dedicated to advancing PEMFC technology, especially over the last few decades, Contributing to its evolution as a promising and impactful solution in the field of clean energy [15]. The schematic diagram of the PEM fuel cell is shown in Figure 1.

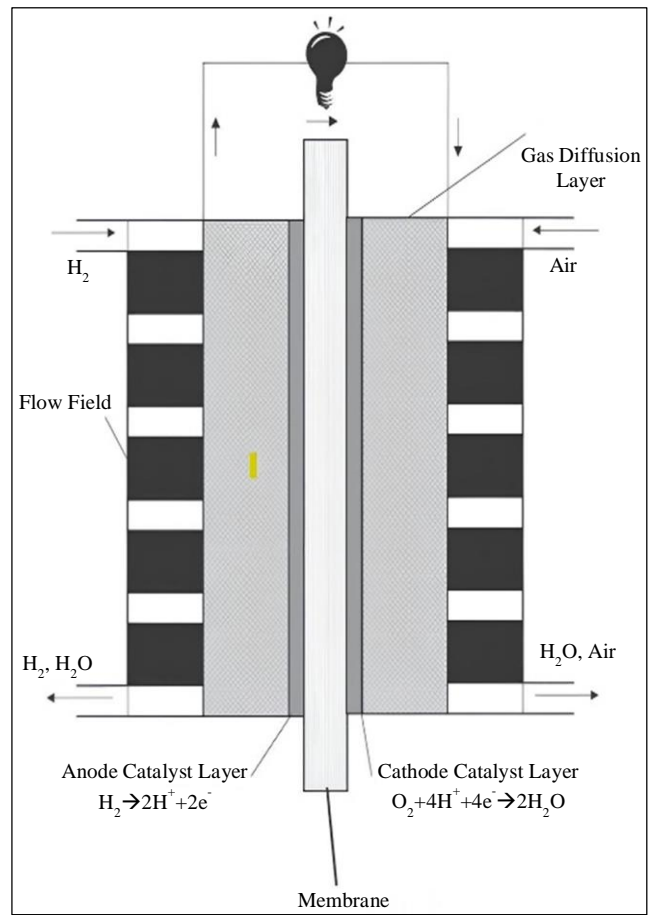


Fig. 1 Schematic diagram of PEM fuel cell [16]

In a PEMFC, the polymer-electrolyte membrane plays a central role by facilitating ion conduction while impeding electron transfer between electrodes. The catalyst layers within the membrane house intricate structures composed of precious metal nanoparticles supported on porous carbon and ionomer, establishing pathways for the transport of reactants, products, electrons and protons to and from active sites where electrochemical reactions take place. The anode is responsible for fuel oxidation when hydrogen is utilized to release protons and electrons. Protons move through the membrane while electrons navigate the external circuit [16].

At the cathode catalyst layer, protons and electrons recombine with oxygen, which results in the production of water. The membrane and electrodes are enclosed between graphite blocks featuring gas flow channels and porous diffusion media to ensure the distribution of gaseous hydrogen and oxygen across electrodes and the completion of the electron flow circuit. These carbon media include a macroporous gas-diffusion layer and a microporous layer adjacent to the catalyst layer, contributing to the efficient functioning of the PEMFC [16].

The stack power ( $P_{stack}$ ) can be calculated by considering the voltage ( $V_{cell}$ ) across a single cell and the current ( $I_{stack}$ ) passing through the stack in account of the number of cells ( $N_{cells}$ ) in the stack. The relationship is given by Ohm's Law:

$$P_{stack} = I_{stack} \times V_{cell} \times N_{cells} \quad (1)$$

The voltage across a single PEMFC ( $V_{cell}$ ) is a function of the actual cell potential ( $E_{cell}$ ), the current passing through the stack ( $I_{stack}$ ) and the internal resistance of the cell ( $R_{int}$ ). This relationship can be expressed as follows:

$$V_{cell} = E_{cell} - I_{stack} \times R_{int} \quad (2)$$

$$E_{cell} = E^0_{cell} - \frac{RT}{nF} \ln\left(\frac{P_{O_2}}{\sqrt{P_{H_2}}}\right) \quad (3)$$

$$I_{stack} = \frac{V_{stack}}{R_{int} + R_{ext}} \quad (4)$$

Where  $E^0_{cell}$  is the standard cell potential, R is the ideal gas constant, T is system temperature, n is the number of electrons involved in the reaction (n=2 in this case),  $R_{ext}$  is the external resistance in the fuel cell circuit, F is Faraday's constant,  $P_{O_2}$  and  $P_{H_2}$  are the partial pressures of air and water vapor respectively.

The reference parameters of the PEMFC stack have been extracted from SIMULINK with 24V and 1.26KW PEMFC, as given in Table 1. The electrical characteristics of the PEMFC Stack with nominal and maximum values of stack voltage, current and power are shown in Figure 2.

Table 1. Description of PEMFC stack

S. No.	Parameter	Value
1	Standard Cell Potential ( $E^0_{cell}$ )	1.115V
2	Ideal Gas Constant (R)	8.314J/(mol·K)
3	System Temperature (T)	328K
4	Faraday's Constant (F)	96,485 C/mol
5	Nominal Utilization of $H_2$ ( $p_{H_2}$ )	99.92%
6	Nominal Utilization of $O_2$ ( $p_{O_2}$ )	1.813%
7	$I_{stack}$ Nominal	52A
8	$I_{stack}$ Maximum	100A
9	$V_{stack}$ Nominal	24.23V
10	$V_{stack}$ Maximum	20V
11	$P_{stack}$ Nominal	1259.96W
12	$P_{stack}$ Maximum	2000W
13	$R_{int}$	0.061871 $\Omega$

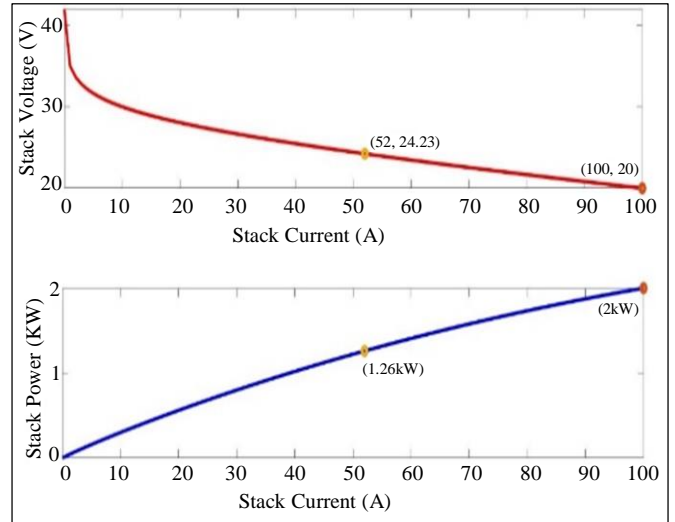


Fig. 2 Electrical characteristics of PEMFC stack

$$\eta(\%) = \frac{P_{OUT}}{P_{IN}} \times 100 \quad (5)$$

Where  $P_{OUT}$  is the electrical power output, and  $P_{IN}$  is the fuel input power.

$P_{IN}$  is calculated by multiplying the nominal consumption of fuel with the Lower Heating Value (LHV) of hydrogen. The efficiency ( $\eta$ ) of the system can then be determined by comparing the useful work output to the input energy:

$$P_{IN} = Q_{IN} = \text{Nominal fuel consumption} \times \text{LHV of hydrogen} \quad (6)$$

The effect of variations in the input sources (air & water pressure and temperature) of the PEMFC stack on the electrical parameters were analyzed using the specific design equations 1,2,3, and 4, respectively. This mathematical analysis is done using the MATLAB code, which effectively simulates fuel cell performance, and the results are consistent with the expected theoretical values.

This helps in analyzing the impact of parameter variations on fuel cell operation and understanding how changes in temperature and gas pressures influence the overall system before integrating with the MPPT controller. The effects of

input sources on the output parameters are shown in Table 2. The PEMFC stack dynamic analysis is simulated for partial variations in air pressure, water pressure and system temperature, as shown in Figures 3, 4 and 5, respectively. It is observed that the impact of partial variations in  $P_{H_2}$  is the inverse of partial variations in  $P_{O_2}$  as shown in simulated outputs of Figures 3 and 4. The inverse relationship observed in the impact of partial variations in  $P_{H_2}$  and  $P_{O_2}$  is a common phenomenon in fuel cells.

Typically, an increase in hydrogen pressure and a decrease in oxygen pressure can have similar effects on fuel cell performance. At the same time, the effect of variations in system temperature is similar to the effect of partial variations in  $P_{H_2}$ , as shown in Figures 4 and 5.

Both hydrogen pressure and system temperature impact the kinetics of the electrochemical reactions occurring in a fuel cell. An increase in either parameter tends to promote more favorable conditions for the reactions to occur efficiently.

**Table 2. Dynamic analysis of the PEMFC stack**

Cell Parameters	$E_{cell}$	$R_{ext}$	$I_{stack}$	$P_{stack}$
Nominal Utilization of $P_{O_2}$ & $P_{H_2}$	1.1717 V	0.4434Ω	47.9517A	1161.86W
5% Reduction in $P_{O_2}$ & 2% Increase in $P_{H_2}$	1.1159 V	0.4445Ω	47.8500A	1159.40W
5.5% (20K) Increase in System Temperature	1.1751V	0.4433Ω	47.9580A	1162.02W

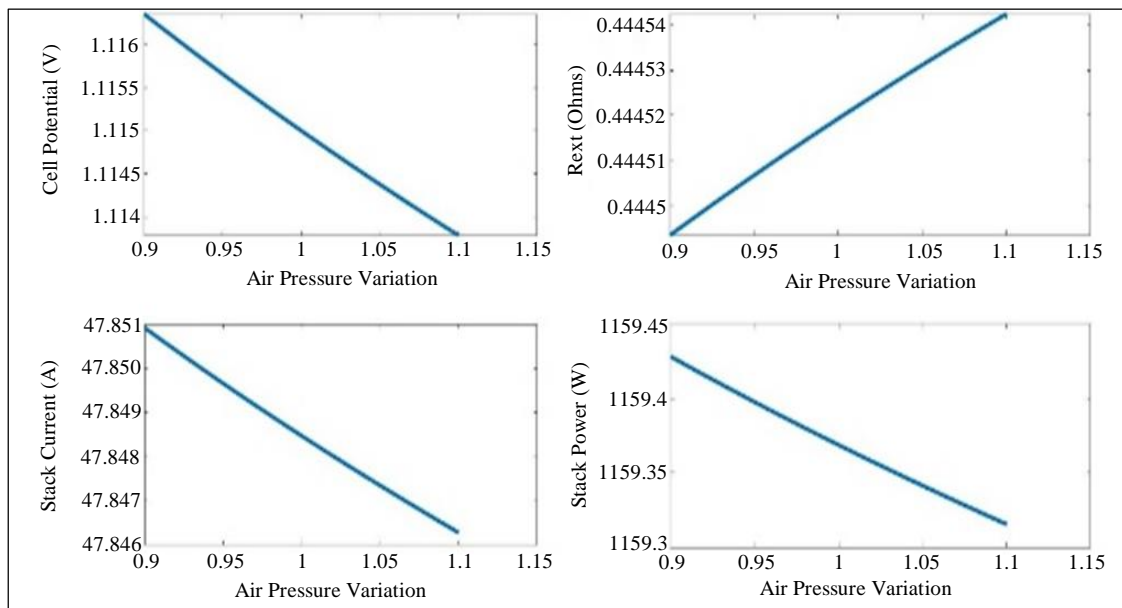


**Fig. 3 PEMFC performance with  $P_{O_2}$  variations**



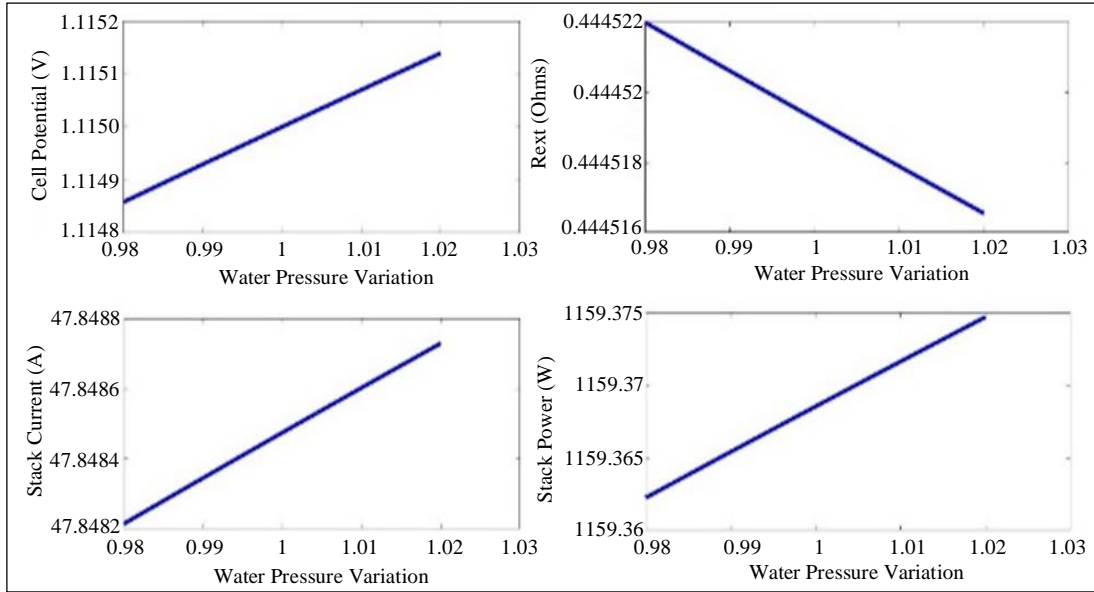


Fig. 4 PEMFC performance with P<sub>H2</sub> variations

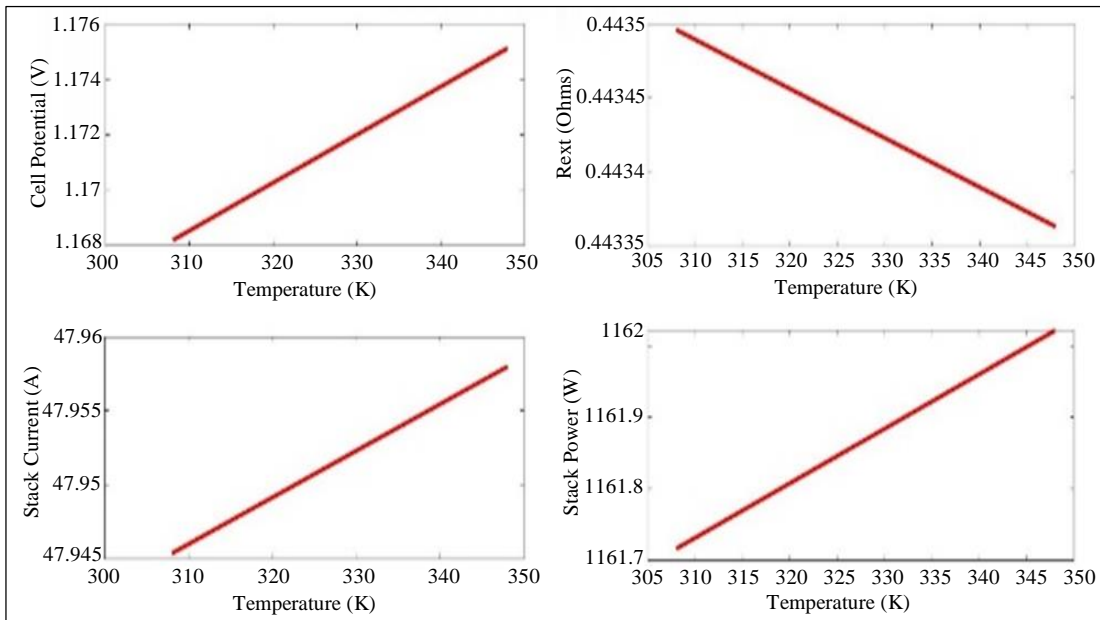


Fig. 5 PEMFC performance with temperature variations

### 2.2. Design of Switched Inductor DC-to-DC Boost Converter

The envisioned SIDC aims to address the specific challenges encountered by standalone PV systems, which grapple with fluctuations in solar irradiance and varying loads.

The fundamental constituents of this converter comprise two inductors ( $L_1$  &  $L_2$ ), two switches ( $M_1$  &  $M_2$ ), the PEMFC as input voltage source ( $V_{PEMFC}$ ), two input capacitors ( $C_1$  &  $C_2$ ), the output capacitor ( $C_{out}$ ), seven diodes and the output load ( $R_L$ ). Together, these components collaborate to facilitate effective power conversion and regulation. Figure 6 illustrates the simulation model of the SIDC converter.

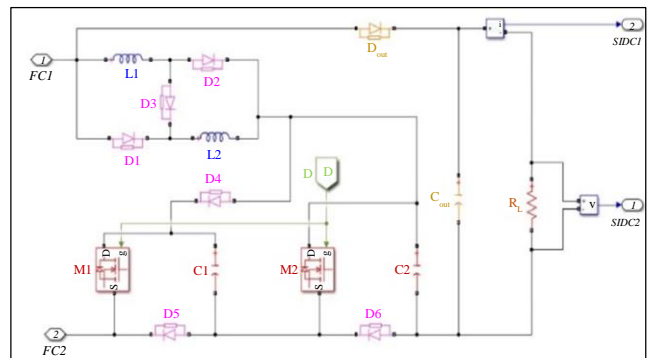


Fig. 6 Simulation diagram of SIDC converter

During Mode 1, both switches  $M_1$  and  $M_2$  in the converter are in the ON state. Diodes  $D_1$ ,  $D_2$ , and  $D_0$  are forward-biased due to the polarity of the inductors and the input voltage source  $V_{in}$ . Inductors  $L_1$  and  $L_2$  are connected in parallel, allowing them to charge simultaneously. Energy is transferred to the inductors from the input voltage source, the energy stored in capacitor  $C_1$  ( $VC_1$ ), and the energy stored in capacitor  $C_2$  ( $VC_2$ ). This energy transfer results in an increase in the current flowing through the inductors. Since  $L_1$  and  $L_2$  are connected in parallel and have the same voltage source, which is denoted as  $VL_1$  and  $VL_2$ , the load connected to the converter is powered by a combination of the input voltage, the voltage across  $C_1$  ( $VC_1$ ), the voltage across  $C_2$  ( $VC_2$ ).

During Mode 2, both switches  $M_1$  and  $M_2$  in the converter are in the OFF state. As a result, the diodes  $D_1$ ,  $D_2$ , and  $D_0$  become reverse-biased and do not conduct current. In contrast, diodes  $D_3$ ,  $D_4$ ,  $D_5$ , and  $D_6$  are forward-biased and allow current to flow through them. This voltage represents the energy stored in the inductors and is an important aspect of the converter's operation. In Mode 2, both inductors  $L_1$  and  $L_2$  are connected in series with each other.

The series configuration causes them to cooperate in discharging their stored energy. The energy stored in the inductors is dissipated into capacitors  $C_1$  and  $C_2$  equally during this mode. Capacitors  $C_1$  and  $C_2$  act as energy storage devices and absorb the energy previously stored in the inductors. During this period, the load is supplied by the energy stored in the capacitor  $C_{out}$ . Capacitor  $C_{out}$  serves as the primary source of power to the load in Mode 2.

The average voltage of the SIDC converter when it is operated in a continuous mode of operation is calculated using reference [17] as given below,

$$\frac{V_{out}}{V_{PEMFC}} = \frac{3-D}{(1-3D)} = \text{voltage transfer ratio} \quad (7)$$

The  $R_L$  is calculated using the  $P_{out}$ , and  $V_{out}$  is given as,

$$R_L = \frac{V_{out}^2}{P_{out}} \quad (8)$$

The voltage across the capacitor ( $C_1$ ) can be calculated as,

$$VC_1 = \frac{1+D}{1-3D} = VC_2 \quad (9)$$

Switching frequency ( $f$ ) of 100 kHz has been chosen. Now, the inductor and its current values can be calculated as given below in reference to [17],

$$L = \frac{V_{PEMFC} + VC_1}{\Delta I_L} * D * f = L_1 = L_2 \quad (10)$$

$$I_L = \frac{1}{1+D} \left( \frac{V_{out}^2}{V_{PEMFC} * R_L} - \frac{D * V_{out}}{R_L} \right) \quad (11)$$

The output capacitance ( $C_{out}$ ) is determined by the desired voltage ripple ( $\Delta V_{out}$  is calculated by considering 1% of  $V_{out}$ ) and the load current ( $I_{out}$ ). Let us consider a reasonable value for  $\Delta V_{out} = 2.2V$  (1% of  $V_{out}$ ),

$$I_{out} = \frac{P_{out}}{V_{out}} \quad (12)$$

$$C_1 = \left( \frac{2I_L + I_{out}}{\Delta VC_1} \right) D * f \quad (13)$$

$$C_2 = \left( \frac{I_{out}}{\Delta VC_2} \right) D * f \quad (14)$$

$$C_{out} = \frac{I_{out} * (1-D)}{\Delta V_{out} * f} \quad (15)$$

The SIDC parameters were found out using the derivations mentioned above and are listed as Duty cycle ( $D$ ) is 0.25464,  $L_1=L_2$  will be 0.005756 H, Inductor current ( $I_{L1=L2}$ ) is 32.2874 A,  $C_1$  is 800048.137 F,  $C_2$  is 52612.3982 F, and  $C_{out}$  will be 1.54e-05 F. The impact of variable PEMFCs output voltage on the SIDCs inductor current is shown in Figure 7. When the input voltage is low, the duty cycle tends to be high. This means that the electronic switch stays on for a longer time during each cycle.

A longer switch-on time allows more energy to flow into the inductor. As a result, the inductor current tends to be higher at low input voltages. Conversely, the duty cycle tends to be low for higher input voltage. This means the switch stays on for a shorter time during each cycle. A shorter switch-on time means less energy flows into the inductor, which leads to a lower inductor current at higher input voltages.

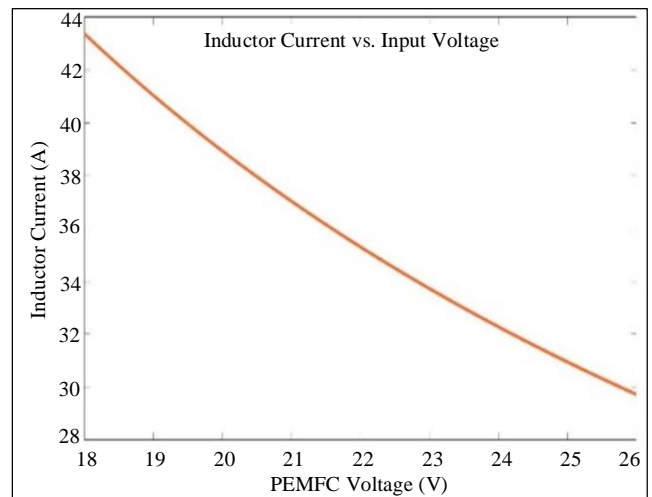


Fig. 7 Inductor current Vs PEMFC voltage

**2.3. Developing an ANFIS Model for MPPT Control**

ANFIS is a hybrid computational model that combines elements of fuzzy logic and neural networks. It is primarily used for modeling complex, nonlinear relationships between input and output data. ANFIS is a type of fuzzy inference system that adjusts its parameters through a learning process, making it capable of adapting to various types of data. The architecture of an ANFIS model typically consists of several layers [17] as follows,

**Input Layer:** The input layer in an ANFIS is the first component of the architecture and serves as the interface between the input data, namely, air pressure ( $P_a$ ) and fuel pressure ( $P_f$ ) and the ANFIS model. Its primary function is to receive the input variables or features and pass them on to the subsequent layers for further processing.

**Fuzzification Layer:** In the fuzzification layer, each input value is mapped to its degree of membership in the fuzzy sets using fuzzy membership functions. The degree of membership ( $\mu$ ) for an input ( $x_i$ ) in a fuzzy set ( $A_i$ ) is calculated using the corresponding membership function (usually Gaussian); the equation for the Gaussian membership function is given as,

$$\mu(A_i) = \exp\left(-\frac{(x_i - c_i)^2}{2\sigma_i^2}\right) \quad (18)$$

**Rule Layer:** The rule layer combines the fuzzy membership values from the fuzzification layer to calculate the firing strength of each rule. If you have "m" rules, you will have "m" firing strengths ( $w_1, w_2, \dots, w_m$ ) for each rule, which can be computed using an aggregation operator (usually minimum), which is given as,

$$w_i = \mu(A_{1i}) \times \mu(A_{2i}) \times \dots \times \mu(A_{ni}) \quad (19)$$

**Consequent Layer:** The consequent layer represents the consequences of each rule. It consists of single-layer neural networks with parameters that need to be learned. For a regression task, the output of each node in the consequent layer ( $y_i$ ) can be calculated as a weighted sum of the firing strengths ( $w_i$ ) with adjustable parameters ( $\theta_i$ ), which is given as,

$$y_i = \theta_0 + \theta_1 \times x_1 + \theta_2 \times x_2 + \dots + \theta_n \times x_n \quad (20)$$

**Output Layer:** The output layer combines the outputs from the consequent layer, typically by taking their weighted sum or applying a specific aggregation method. For a single-output ANFIS, it is often a simple sum which is given as,

$$\text{output} = \frac{\sum(y_i \times w_i)}{\sum w_i} \quad (21)$$

**Learning Algorithm:** ANFIS uses a learning algorithm to adjust its parameters ( $\theta_i$ ) to minimize a predefined error or loss

function. This is typically done using gradient descent or other optimization techniques. The specific equations for parameter updates depend on the chosen optimization method. ANFIS combines the advantages of two Artificial Intelligence techniques (FLC and ANN) into a single model [17]. An ANFIS works by implementing Artificial Neural Network learning methods to tune the parameters of a Fuzzy Inference System (FIS), and the architecture of ANFIS is given in Figure 8.

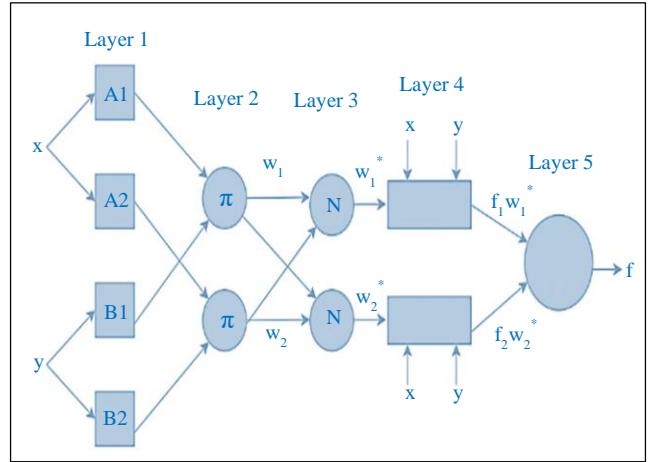


**Fig. 8 ANFIS architecture**

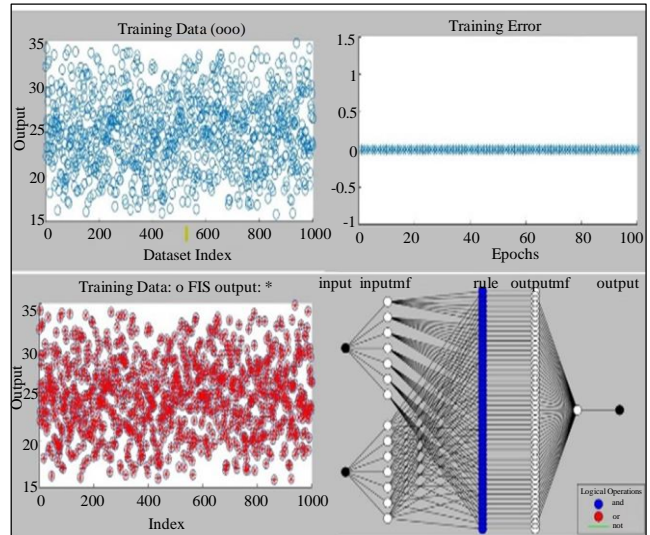


**Fig. 9 Process and architecture of ANFIS**

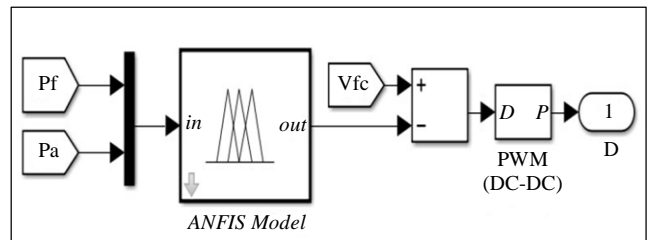


**Fig. 10 SIMULINK model of ANFIS**



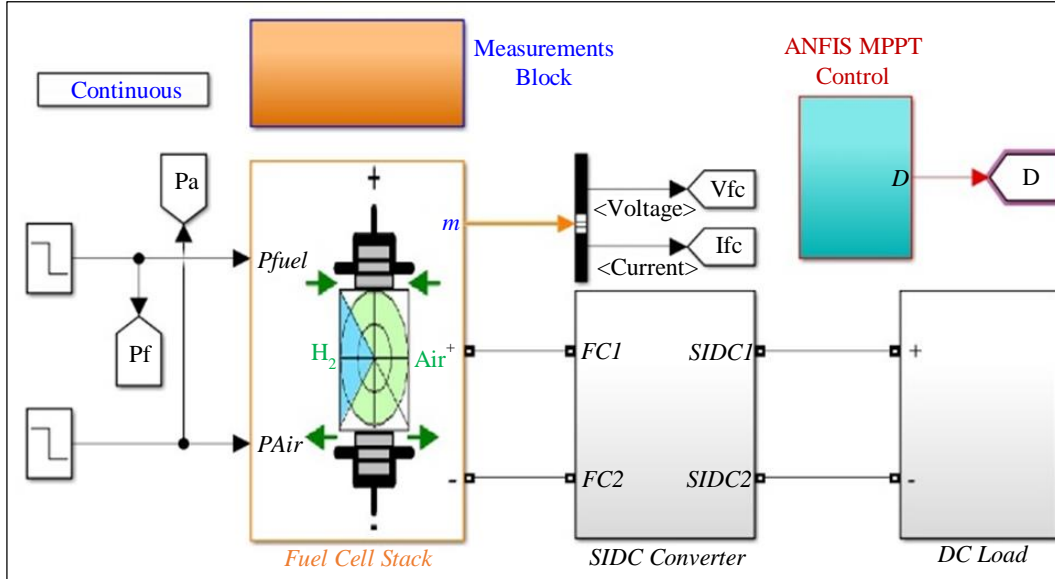


Fig. 11 SIMULINK model of proposed system

### 3. Performance Analysis

#### 3.1. SIDC Converter Output Analysis Using ANFIS Model at STC

The analysis involves utilizing an ANFIS model to examine the output of a PEMFC at STC. This includes the analysis of PEMFC voltage, current and power at STC, as shown in Figure 12. Additionally, the analysis extends to the SIDC converter, encompassing voltage, current and power at STC, as shown in Figure 13.

#### 3.2. Dynamic Analysis of ANFIS and ANN MPPT Control

The simulation involved observing the PEMFC stack's voltage, current and power in response to a decrease in system

temperature at 0.3 seconds and an increase in temperature at 0.6 seconds, as shown in Figure 14.

Both ANFIS and ANN MPPT control methods were employed. The findings indicate that ANFIS exhibits superior stability compared to ANN in response to temperature variations. It is illuminated how the MPPT control algorithm implemented in ANFIS contributes to its heightened stability during temperature changes. Similarly, the analysis extended to changes in air and fuel pressure at 0.3 and 0.6 seconds. ANFIS consistently outperformed ANN in maintaining stability under varying pressure conditions which is shown as simulated results in Figure 15.

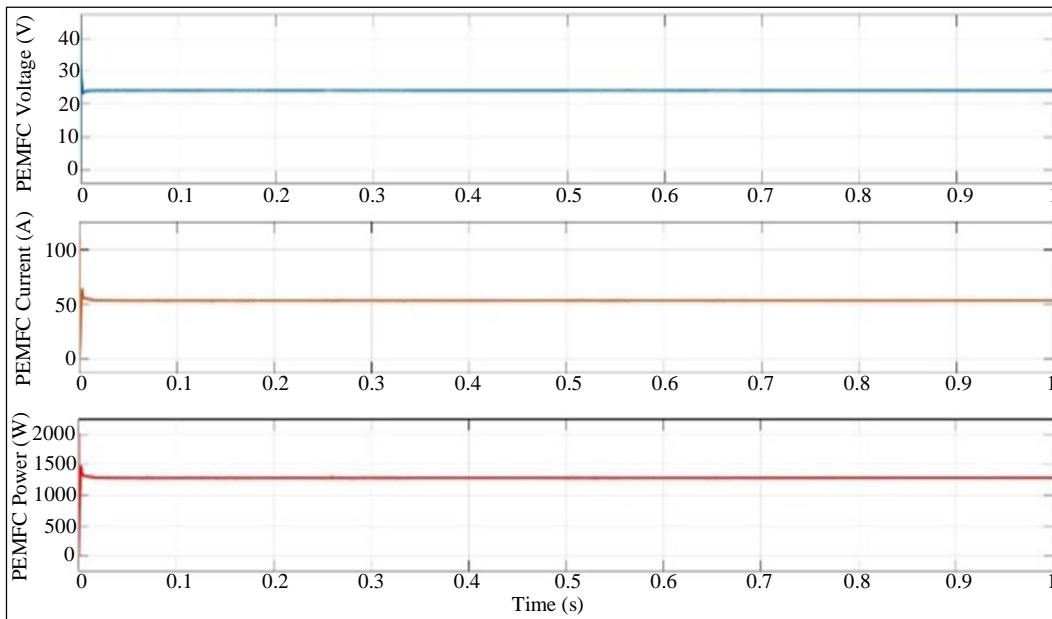


Fig. 12 PEMFC performance at STC

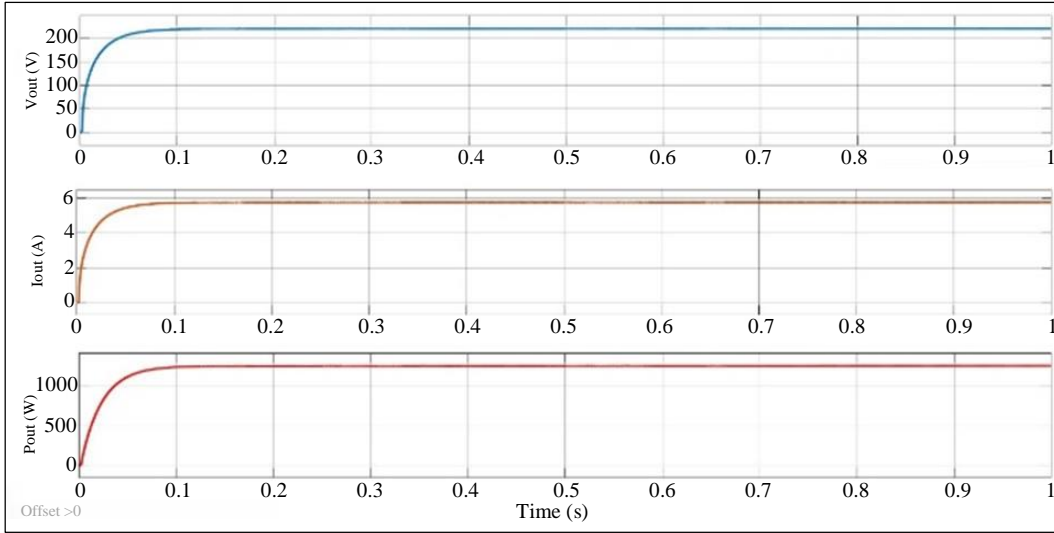


Fig. 13 SDC performance at STC

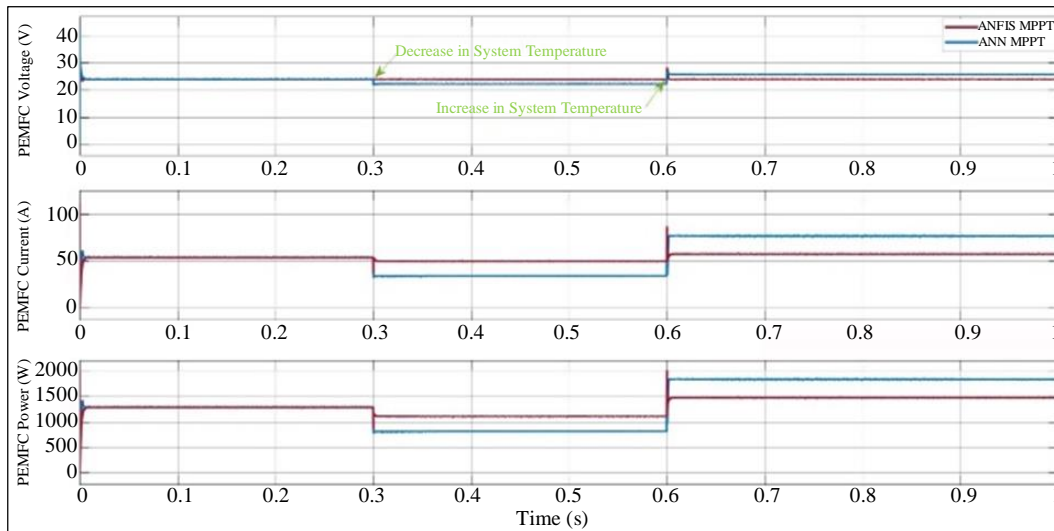


Fig. 14 PEMFC performance for change in system temperature

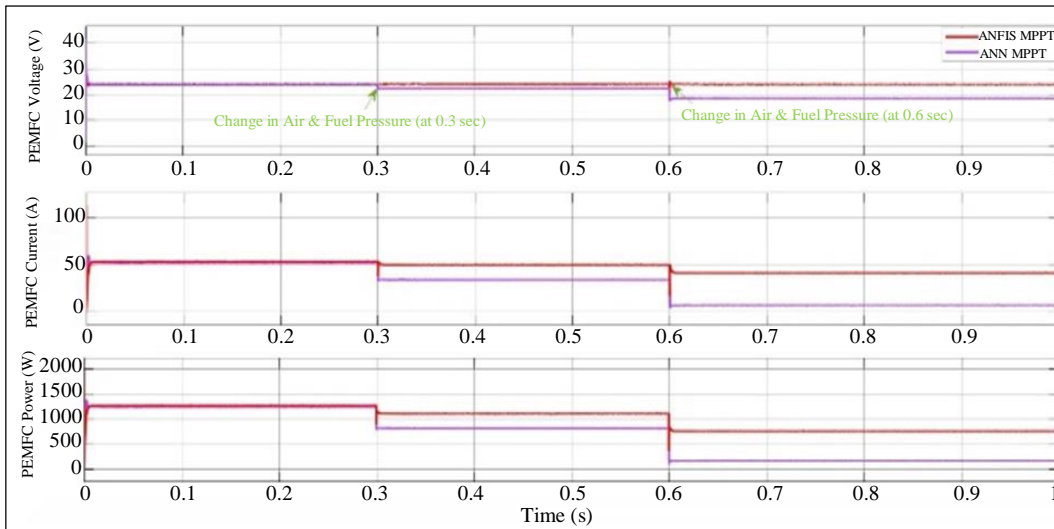


Fig. 15 PEMFC performance for change in air and fuel pressure

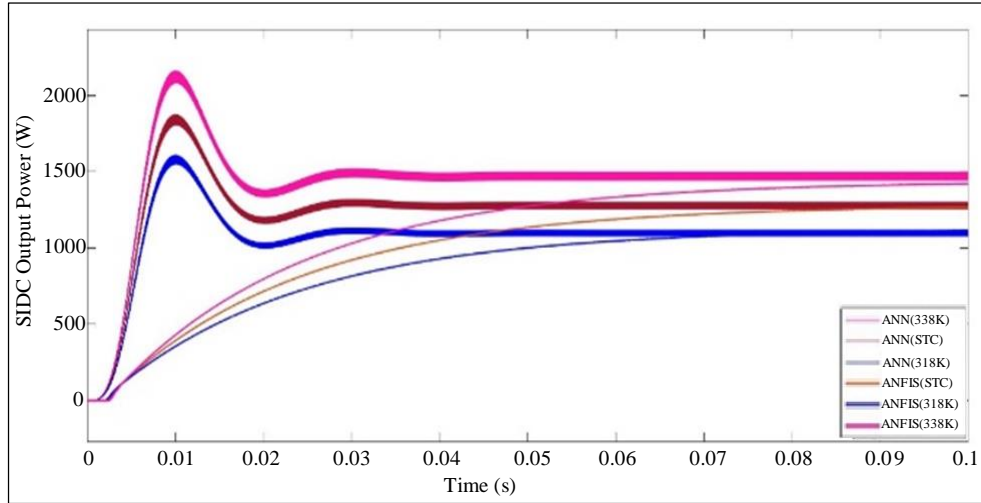


Fig. 16 SIDC performance for change in system temperature

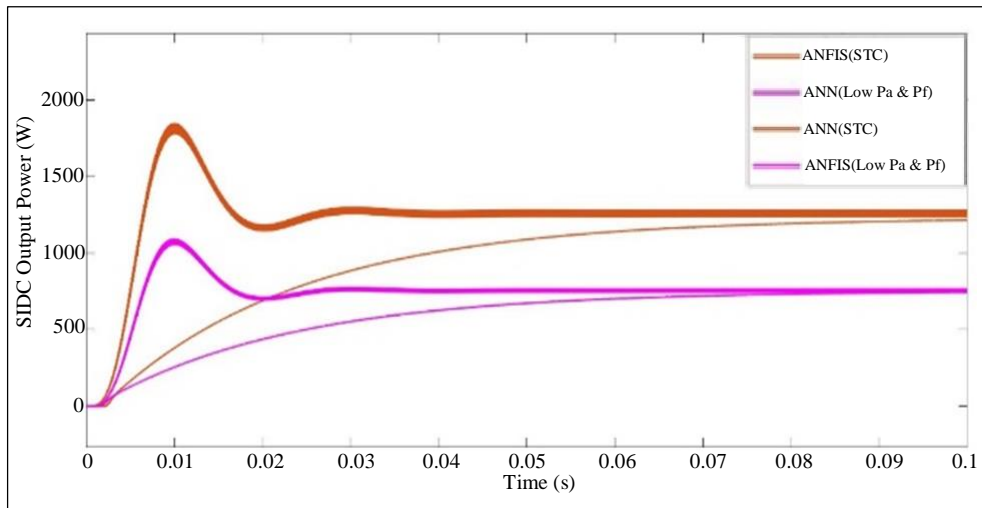


Fig. 17 SIDC performance for change in air and fuel pressure

In the analysis of the SIDC converter, it is observed that the output voltage's response to changes in system temperature, air pressure and fuel pressure. The temperature at STC was 328K, with a decrease to 318K and an increase to 338K during the simulation. The SIDC converter showcased varying output voltages in response to these temperature fluctuations, as shown in Figure 16. Our study affirms the superior stability of ANFIS over ANN in controlling the SIDC converter under dynamic temperature conditions. Additionally, the analysis extended to changes in air and fuel pressure, revealing the robust performance of ANFIS in maintaining stability across diverse environmental scenarios, as shown in Figure 17. These findings underscore the potential of ANFIS for effective control in SIDC converters, especially under temperature and pressure variations.

#### 4. Conclusion

In conclusion, this study presents a comprehensive investigation into the integration of an ANFIS for MPPT in a

1.26 kW, 24V PEMFC system coupled with a switched inductor DC-to-DC boost converter. Our research encompasses the modeling of the PEMFC system, the design of the boost converter and the development of an ANFIS model for MPPT control. Simulations conducted under varying air and water pressure conditions and temperature fluctuations reveal the dynamic behavior of the PEMFC system. The comparative analysis between ANFIS and ANN based MPPT control for the switched inductor converter highlights the superior stability of ANFIS, particularly in response to temperature and pressure variations.

Notably, the findings demonstrate that the ANFIS-based MPPT control algorithm contributes to heightened stability during dynamic environmental changes. The analysis of the SIDC converter output under diverse conditions affirms the robust performance of ANFIS, showcasing its effectiveness in maintaining stability amidst temperature and pressure fluctuations.

Our study underscores the potential of ANFIS as an advanced control strategy for SIDC converters, with implications for optimizing fuel cell systems under varying operating conditions. The outcomes of this research provide valuable insights into the dynamic behavior of PEMFC systems, emphasizing the significance of advanced control strategies for enhancing performance. The proposed model and control strategies contribute to the advancement of PEMFC technology, offering a solid foundation for the design and optimization of fuel cell systems in real-world environmental scenarios. As the global interest in renewable energy sources continues to grow, our work aligns with the evolving landscape of sustainable energy solutions.

In conclusion, the effectiveness of ANFIS in optimizing the SIDC converter output underlines its potential for practical implementation in fuel cell systems, marking a significant step forward in the pursuit of efficient and stable renewable energy solutions.

### Acknowledgement

We gratefully acknowledge the support and facilities provided by the authorities of the Annamalai University, Annamalai Nagar, Tamilnadu, India, to carry out this research. We would also like to thank our supporting staff from Annamalai University, who gave insight and knowledge that considerably aided the research.

### References

- [1] Miriam M. Tellez-Cruz et al., "Proton Exchange Membrane Fuel Cells (PEMFCs): Advances and Challenges," *Polymers*, vol. 13, no. 18, pp. 1-54, 2021. [[CrossRef](#)] [[Google Scholar](#)] [[Publisher Link](#)]
- [2] Alexander Kraysberg, and Yair Ein-Eli, "Review of Advanced Materials for Proton Exchange Membrane Fuel Cells," *Energy & Fuels*, vol. 28, no. 12, pp. 7303-7330, 2014. [[CrossRef](#)] [[Google Scholar](#)] [[Publisher Link](#)]
- [3] Norazlianie Sazali et al., "New Perspectives on Fuel Cell Technology: A Brief Review," *Membranes*, vol. 10, no. 5, pp. 1-18, 2020. [[CrossRef](#)] [[Google Scholar](#)] [[Publisher Link](#)]
- [4] Yun Wang et al., "Materials, Technological Status, and Fundamentals of PEM Fuel Cells - A Review," *Materials Today*, vol. 32, pp. 178-203, 2020. [[CrossRef](#)] [[Google Scholar](#)] [[Publisher Link](#)]
- [5] Christopher Herwerth et al., "Development of a Small Long Endurance Hybrid PEM Fuel Cell Powered UAV," SAE Technical Paper, pp. 1-10, 2007. [[CrossRef](#)] [[Google Scholar](#)] [[Publisher Link](#)]
- [6] Ephraim Bonah Agyekum et al., "Research Progress, Trends, and Current State of Development on PEMFC-New Insights from a Bibliometric Analysis and Characteristics of Two Decades of Research Output," *Membranes*, vol. 12, no. 11, pp. 1-33, 2022. [[CrossRef](#)] [[Google Scholar](#)] [[Publisher Link](#)]
- [7] Kui Jiao et al., "Designing the Next Generation of Proton-Exchange Membrane Fuel Cells," *Perspectives*, vol. 595, pp. 361-369, 2021. [[CrossRef](#)] [[Google Scholar](#)] [[Publisher Link](#)]
- [8] Linda Ager-Wick Ellingsen et al., "Nanotechnology for Environmentally Sustainable Electromobility," *Nature Nanotechnology*, vol. 11, pp. 1039-1051, 2016. [[CrossRef](#)] [[Google Scholar](#)] [[Publisher Link](#)]
- [9] Nisa Nur Atak, Battal Dogan, and Murat Kadir Yesilyurt, "Investigation of the Performance Parameters for a PEMFC by Thermodynamic Analyses: Effects of Operating Temperature and Pressure," *Energy*, vol. 282, 2023. [[CrossRef](#)] [[Google Scholar](#)] [[Publisher Link](#)]
- [10] Saad Motahhir, Aboubakr El Hammoumi, and Abdelaziz El Ghzizal, "The Most Used MPPT Algorithms: Review and the Suitable Low-Cost Embedded Board for Each Algorithm," *Journal of Cleaner Production*, vol. 246, 2020. [[CrossRef](#)] [[Google Scholar](#)] [[Publisher Link](#)]
- [11] Liping Fan, and Xianyang Ma, "Maximum Power Point Tracking of PEMFC Based on Hybrid Artificial Bee Colony Algorithm with Fuzzy Control," *Scientific Reports*, vol. 12, pp. 1-12, 2022. [[CrossRef](#)] [[Google Scholar](#)] [[Publisher Link](#)]
- [12] Abdelfatah Kolli et al., "A Review on DC/DC Converter Architectures for Power Fuel Cell Applications," *Energy Conversion and Management*, vol. 105, pp. 716-730, 2015. [[CrossRef](#)] [[Google Scholar](#)] [[Publisher Link](#)]
- [13] W.R.W. Daud et al., "PEM Fuel Cell System Control: A Review," *Renewable Energy*, vol. 113, pp. 620-638, 2017. [[CrossRef](#)] [[Google Scholar](#)] [[Publisher Link](#)]
- [14] Pascal Kuate Nkounhawa, Dieunedort Ndapeu, and Bienvenu Kenmeugne, "Artificial Neural Network (ANN) and Adaptive Neuro-Fuzzy Inference System (ANFIS): Application for a Photovoltaic System under Unstable Environmental Conditions," *International Journal of Energy and Environmental Engineering*, vol. 13, pp. 821-829, 2022. [[CrossRef](#)] [[Google Scholar](#)] [[Publisher Link](#)]
- [15] Yun Wang et al., "A Review of Polymer Electrolyte Membrane Fuel Cells: Technology, Applications, and Needs on Fundamental Research," *Applied Energy*, vol. 88, no. 4, pp. 981-1007, 2011. [[CrossRef](#)] [[Google Scholar](#)] [[Publisher Link](#)]
- [16] Adam Z. Weber, Sivagaminathan Balasubramanian, and Prodip K. Das, "Chapter 2 Proton Exchange Membrane Fuel Cells," *Advances in Chemical Engineering*, vol. 41, pp. 66-144, 2012. [[CrossRef](#)] [[Google Scholar](#)] [[Publisher Link](#)]
- [17] Ahmed Al-Hmouz et al., "Modeling and Simulation of an Adaptive Neuro-Fuzzy Inference System (ANFIS) for Mobile Learning," *IEEE Transactions on Learning Technologies*, vol. 5, no. 3, pp. 226-237, 2012. [[CrossRef](#)] [[Google Scholar](#)] [[Publisher Link](#)]